Preprints (www.preprints.org) | NOT PEER-REVIEWED | Posted: 16 May 2023 doi:10.20944/preprints202305.1142.v1

Disclaimer/Publisher's Note: The statements, opinions, and data contained in all publications are solely those of the individual author(s) and contributor(s) and not of MDPI and/or the editor(s). MDPI and/or the editor(s) disclaim responsibility for any injury to people or property resulting from any ideas, methods, instructions, or products referred to in the content.

Thermally Stable and Reusable Silica and Nano-fructosome Encapsulated CalB enzyme Particles for Rapid Enzymatic Hydrolysis and Acylation

Woo Young Jang[1], Jung Hoon Sohn[2] and Jeong Ho Chang[1,*]

[1]Korea Institute of Ceramic Engineering and Technology, Chungbuk, 28160, Korea
[2]Korea Research Institute of Bioscience and Biotechnology, Daejeon, 34141, Korea (E-mail: jhchang@kicet.re.kr)
* Correspondence: author. ***E-mail address:*** jhchang@kicet.re.kr (J.H. Chang). ***Phone:*** +82 43 913 1510

Abstract: This study reports the preparation of silica and nano-fructosome encapsulated *Candida antarctica* lipase B particles (CalB@NF@SiO_2) and demonstration of their enzymatic hydrolysis and acylation. CalB@NF@SiO_2 particles were prepared as a function of TEOS concentration (3-100 mM). Their mean particle size was 185 nm by TEM. Enzymatic hydrolysis was performed to compare catalytic efficiencies of CalB@NF and CalB@NF@SiO_2. Catalytic constants (K_m, V_{max}, and K_{cat}) of CalB@NF and CalB@NF@SiO_2 were calculated with Michaelis-Menten equation and Line-weaver Burk plot. Optimal stability of CalB@NF@SiO_2 was found at pH 8 and temperature of 35 ℃. Moreover, CalB@NF@SiO_2 particles were reused for seven cycles to evaluate their reusability. In addition, enzymatic synthesis of benzyl benzoate was demonstrated by an acylation reaction with benzoic anhydride. The efficiency of CalB@NF@SiO_2 for converting benzoic anhydride to benzyl benzoate by the acylation reaction was 97%, indicating that benzoic anhydride was almost completely converted to benzyl benzoate. Consequently, CalB@NF@SiO_2 particles are better than CalB@NF particles for enzymatic synthesis. In addition, they are reusable with high stability at optimal pH and temperature.

Keywords: thermal stability; reusability; silica; encapsulation; nano-fructosome

1. Introduction

Biocatalysts are used in various industries such as medicine, pharmaceuticals, cosmetics, and agriculture due to their substrate specificity, optical selectivity, and involvement in various chemical reactions within the body [1-7]. *Candida antarctica lipase* B (CalB) is a biocatalyst that belongs to the class of enzymes involved in catalyzing reactions. It has high activity and regioselectivity. Depending on reaction conditions, CalB can promote reactions such as hydrolysis and acidolysis [8-12]. CalB is expected to be a non-toxic and renewable energy source. It has the highest catalytic activity at neutral pH and 45 ℃ [13-15]. However, CalB has limitations that hinder its widespread commercial use. CalB is water-soluble, which makes it highly sensitive to organic solvents, leading to reduced reaction efficiency [16,17]. Furthermore, it is difficult to store CalB for a long time. Its storage life is short, resulting in high costs in production and processing stages. In particular, it is difficult to maintain the structural stability of proteins during biochemical reactions, which can affect biological activity the most. Therefore, research on enzyme immobilization, which can complement shortcomings of CalB, is being actively conducted [18-25].

Levan, known as a fructose polymer, is a natural bio-polymer found in small amounts in some plants and microorganisms. Levan has a cationic property in an aqueous solution due to carboxyl and hydroxyl groups of its constituent substance fructose, contributing to its very stable shape. Levan is a functional material that is used in various industries such as functional cosmetics, agriculture, and industry because it is a water-soluble fructose polymer that melts not only at high temperatures, but also at low temperatures [26-28].

© 2023 by the author(s). Distributed under a Creative Commons CC BY license.

Preprints (www.preprints.org) | NOT PEER-REVIEWED | Posted: 16 May 2023 doi:10.20944/preprints202305.1142.v1

Therefore, levan encapsulated enzymes or proteins have been studied and utilized to solve problems of reduced activities of proteinaceous substances such as enzymes. In addition, they are resistant to organic solvents [29-32]. Furthermore, we developed carboxymethyl levan (CML)-based nanocomposites dubbed 'nanofructosome (NF)' and demonstrated effects of NF particles by entrapping lipase [33]. However, these levan encapsulated enzyme complexes are still inherently denatured during long-term storage with poor acid and heat resistance, resulting in reduced catalytic activity. In addition, because it is a water-soluble fructose polymer that melts even at low temperatures, it is difficult to use it in continuous processes as an industrial catalyst. To overcome these limitations, more advanced immobilization techniques are needed.

Silica encapsulation technology is widely known as a method that can efficiently embed materials for industrial purposes [34-36]. The material encapsulated with silica is subordinated to the insoluble support, allowing multiple uses in a continuous process. As a result, it is acid-resistant and heat-resistant, reducing sensitivity to environmental factors and contributing to high efficiency. In addition, it enables long-term storage even at room temperature, effectively reducing the cost of industrial processes. Encapsulation technology using silica has recently been proven to be an effective method for enzyme encapsulation [37-41]. Therefore, it is expected that silica immobilization technology can also be applied to protein-levan complexes. Research is needed to effectively multi-use water-soluble enzymes in organic solvents.

In this study, the enzyme activity of native CalB immobilized via levan (Nano-fructose CalB, CalB@NF) to be used in organic solvents was stabilized under various environmental factors by encapsulating it using tetraethyl orthosilicate (TEOS), a silica precursor. CalB@NF@SiO_2 particles were produced as a function of TEOS concentration ranging from 3-100 mM. The encapsulation morphology of CalB@NF@SiO_2 was confirmed through TEM. Its catalytic activity and reusability were evaluated at various pH and temperature ranges compared to native CalB and CalB@NF. The enzyme amount of CalB@NF@SiO_2 was confirmed through Bradford assay and TGA analysis. Catalytic parameters such as K_m, V_{max}, and K_{cat} were calculated using Michaelis-Menten equation and Line-weaver Burk plot and confirmed through enzymatic hydrolysis using p-nitrophenyl butyrate (PNPB). Enzymatic synthesis was conducted through synthesis of benzyl benzoate using benzoic anhydride. The efficiency of converting benzoic anhydride to benzyl benzoate was calculated.

2. Experimental

2.1. Materials

Candida antarctica lipase B (Native CalB) and CalB@NF were obtained from Korea Research Institute of Bioscience and Biotechnology (33 kDa, Korea) used in encapsulation. Tetraethyl orthosilicate (99%, TEOS), Oleic acid, Iepal CO-520, *p*-nitrophenyl butyrate (98%, PNPB), bovine serum albumin (BSA), Coomassie brilliant blue G-250, phosphoric acid, tris base, phosphate buffer saline (PBS), sodium acetate, glacial acetic acid, benzoic anhydride, and benzyl alcohol were purchased from Sigma-Aldrich (Korea). Cyclohexane, ammonia solution (28-30%), ethanol (99%), methanol, hydrochloric acid, and n-hexane were purchased from Deaejung (Korea). Ethyl ether was provided by J.T.Baker (U.S).

2.2. Preparation of silica encapsulated CalB@NF (CalB@NF@SiO_2)

CalB@NF@SiO_2 particles were prepared with a sol-gel method [41]. Oleic acid (2 mL, solution A), Igepal CO-520 (24 g, solution B), and CalB@NF (90 mg, solution C) were mixed with cyclohexane (100, 300, and 20 mL, respectively). After adding solution A and solution C to solution B, TEOS of various concentrations (3-100 mM) was added drop-wise and stirred for 1 hr. Then 163 mL of ammonia solution was added and stirred for 20 hr. After stirring was complete, 325 mL of methanol was added. After confirming precipitate was formed, the supernatant was then removed. The precipitate was washed three times with n-hexane and completely vacuum dried at room temperature.

Preprints (www.preprints.org) | NOT PEER-REVIEWED | Posted: 16 May 2023 doi:10.20944/preprints202305.1142.v1

2.3. Quantification of enzymes in native CalB, CalB@NF, and CalB@NF@SiO₂

The amount of entrapped enzyme was determined by Bradford assay using a protein reagent [42,43]. The protein reagent was prepared as follows. First, add 50 mL of ethanol and 100 mg of Coomassie brilliant blue G-250 into a 1 L volumetric flask. After adding 100 mL of 85% (w/v) phosphoric acid, distilled water was added to have a final volume of 1 L. The enzyme content was evaluated based on standard solutions and estimated by comparing concentration differences. BSA was used as a standard. The absorbance was measured at 595 nm by UV-Visible spectrophotometry.

2.3. pH and thermal stability of native CalB, CalB@NF, and CalB@NF@SiO₂

Effects of pH and temperature on stability of native CalB, CalB@NF, and CalB@NF@SiO_2 were determined based on their catalytic activities using PNPB at various pH (0.1 M of sodium acetate for pH 5-6 and 0.1 M of tris-HCl for pH 7-9) and temperature (5-65 °C) conditions. After 0.1 mg/mL of native CalB, CalB@NF, or CalB@NF@SiO_2 was added to the substrate solution, catalytic activities were calculated at optimum pH and temperature conditions.

2.5. Reusability of native CalB, CalB@NF, and CalB@NF@SiO₂

Reusability of native CalB, CalB@NF, and CalB@NF@SiO_2 was evaluated in repeated cycles with PNPB. First, 0.1 mg/mL of native CalB, CalB@NF, or CalB@NF@SiO_2 was added into the substrate solution. Nnative CalB, CalB@NF, and CalB@NF@SiO_2 were then recovered from reaction medium by centrifugation at 15,000 rpm for 1 min and washed with 0.1 M of tris-HCl buffer (pH 7.4) to remove any residual substrate. The process was evaluated up to 7 cycles to examine reusability of each catalyst. The absorbance was measured at 400 nm by UV-Visible spectrophotometry.

2.6. Enzymatic hydrolysis for p-nitrophenyl butyrate with native CalB, CalB@NF, and CalB@NF@SiO₂

Enzymatic hydrolysis against PNPB was achieved with native CalB, CalB@NF, or CalB@NF@SiO_2. PNPB solution at 0.1 M was prepared and diluted to different concentrations (0.0625-1.0 mM) with 0.1 M of tris-HCl buffer (pH 7.4). After 0.1 mg/mL of native CalB, CalB@NF, or CalB@NF@SiO_2 was added into substrate solution, the mixture was centrifuged at 15,000 rpm for 1 min. The absorbance of the product, *p*-nitrophenol (PNP), was measured at 400 nm by UV-Visible spectrophotometry. Catalytic parameters such as Michaelis-Menten constant (K_m), maximum reaction velocity (V_{max}), and turnover value (K_{cat}) were calculated for native CalB, CalB@NF, and CalB@NF@SiO_2.

2.7. Enzymatic synthesis for benzyl benzoate with native CalB, CalB@NF, and CalB@NF@SiO₂

Enzymatic synthesis of benzyl benzoate proceeded through an acylation reaction by mixing 10 mL of benzoic anhydride and 2.26 g of benzyl alcohol. After 0.5 g of native CalB, CalB@NF, or CalB@NF@SiO_2 was added, the mixture was incubated at 50 °C for 24 h. After the reaction was completed, the supernatant was separated by centrifugation at 2,500 rpm for 5 min. Separated supernatants were then subjected to column chromatography. The solvent was evaporated using a rotary evaporator after thin layer chromatography (TLC) analysis. The production of benzyl benzoate was confirmed by measuring absorbance at 229 nm using UV-Visible spectrophotometry.

28. Characterizations

Transmitted morphological details of the prepared CalB@NF@SiO_2 according to TEOS concentration were evaluated with a JEM-2100Plus transmission electron microscope (TEM) (JEOL, Japan) at an accelerating voltage of 200 kV. Overall morphological details were analyzed with a TESCAN MIRA3 field emission scanning electron microscopy (FE-SEM) (TESCAN, Czech) operated at 2 kV. To evaluate the amount of enzyme encapsulated in CalB@NF@SiO_2, thermogravimetric analysis (TGA) at 700 °C (10 °C/min)

Preprints (www.preprints.org) | NOT PEER-REVIEWED | Posted: 16 May 2023 doi:10.20944/preprints202305.1142.v1

in a nitrogen atmosphere was performed with a Q600 TA instrument (Waters, USA). Fourier transform infrared (FT-IR) was performed with the KBr method using Frontier (Perkinelmer, US) for characterization of CalB@NF@SiO_2. UV-Visible spectrophotometry was performed using a Mega 900 (SCINCO, Korea) instrument at 190–500 nm. Column chromatography was performed on silica gel with a pore size of 60 Å and a particle size of 32-63 nm. After separation, the reaction was confirmed by thin chromatography (TLC) visualized with 240 nm UV light on Merck silica gel 60 F254 plates.

3. Results and discussion

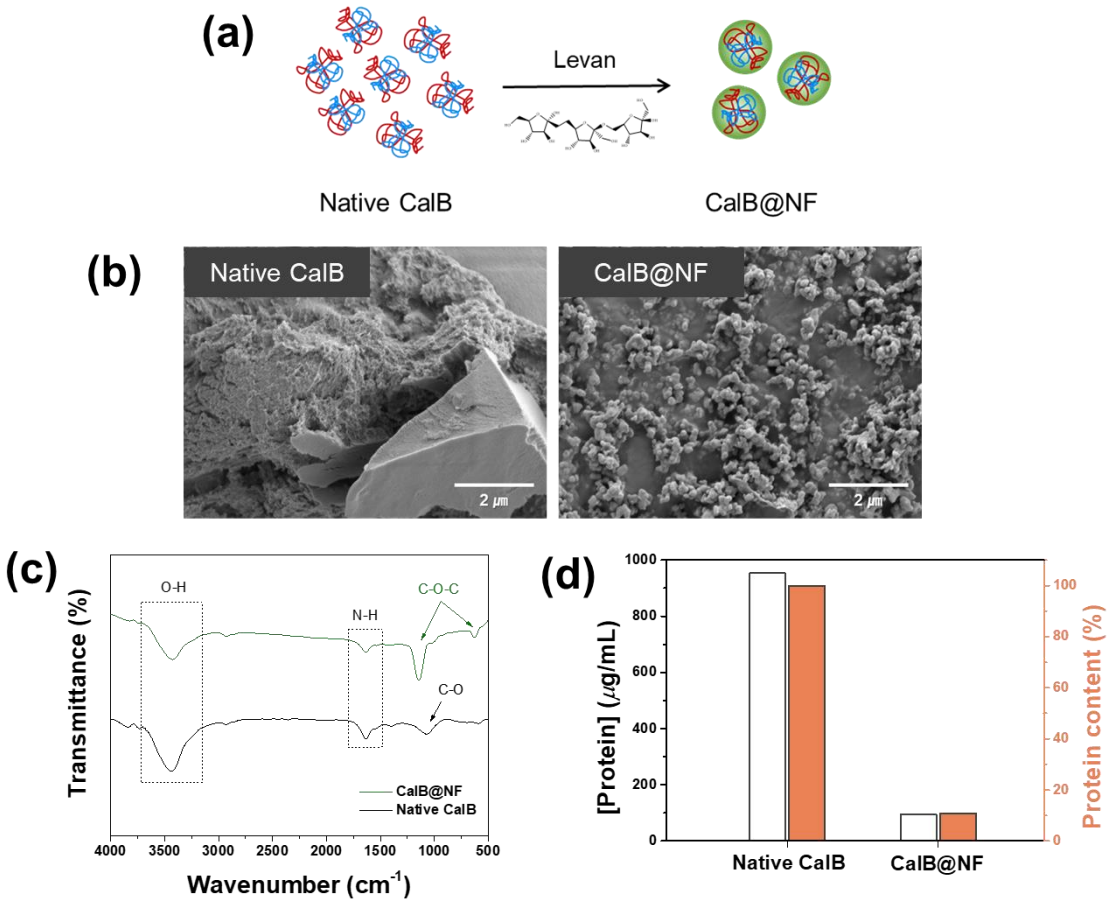

.

Figure 1. (a) CalB@NF preparation process with levan, (b) FE-SEM images, (c) FT-IR spectrum, and (d) protein quantification of native CalB and CalB@NF by Bradford assay.

Fig. 1 shows a comparison of native CalB and CalB@NF. CalB@NF was inserted into levan, a fructose polymer, as shown in Fig. 1(a). CalB@NF was a complex formed by trapping protein inside a nanoparticle. The protein was simply trapped without forming a chemical bond with the levan nanoparticle. Morphological details of native CalB and CalB@NF are shown in Fig. 1(b). Native CalB had no specific shape, while CalB@NF particles were spherical in shape with a mean size of 150 nm. Fig. 1(c) shows FT-IR spectra of native CalB and CalB@NF. Both samples showed common O-H stretching vibration at 3500 cm^{-1} and N-H bending at 1635 cm^{-1}. In addition, anti-symmetric stretching of C-O-C and C-O-C aromatics bending was observed at 1150 cm^{-1} and 630 cm^{-1} for CalB@NF due to the chemical bond of levan. These results indicated that native CalB was well inserted into levan in CalB@NF by C-O-C bending of levan. Fig. 1(d) shows amounts of CalB enzyme in native CalB and CalB@NF determined by the Bradford assay. Amounts of CalB

Preprints (www.preprints.org) | NOT PEER-REVIEWED | Posted: 16 May 2023 doi:10.20944/preprints202305.1142.v1

enzyme for native CalB and CalB@NF at the same weight were 953.5 μg/mL and 94.7 μg/mL, respectively. Therefore, CalB@NF contained 10 times less protein than native CalB. To enable CalB@NF, in which the CalB enzyme was inserted into levan, to be used efficiently in industrial processes under various environmental conditions and for long-term storage at room temperature, silica encapsulation was performed to maintain a stable catalytic activity.

CalB@NF@SiO_2 was prepared by adjusting the TEOS concentration for CalB@NF in the range of 3-100 mM as shown in Fig. 2(a). The morphology of the prepared CalB@NF@SiO_2 was confirmed by FE-SEM and TEM for each TEOS concentration as shown in Figs. 2(b) and 2(c). CalB@NF@SiO_2 had a spherical shape. It became more uniform as the concentration of TEOS increased. Average sizes of particles prepared with TEOS concentrations of 0, 3, 5, 10, 20, 30, 50, and 100 mM were 150, 308, 186, 149, 35, 47, 52, and 66 nm, respectively. As shown in Fig. 2(c), a silica shell was obtained at TEOS concentrations of 3, 5, and 10 mM, but not obtained at TEOS concentration of 0 mM, proving successful encapsulation. Moreover, only normal silica was observed at TEOS concentration of 20 mM or higher. As shown in Fig. 2(b), when TEOS was 20 mM or more, the average particle size was much smaller than that when TEOS concentration was 0 mM, indicating that CalB@NF was not encapsulated. This result was because excessive TEOS concentration in the sol-gel reaction could cause silanols generated by hydrolysis to undergo a condensation reaction.

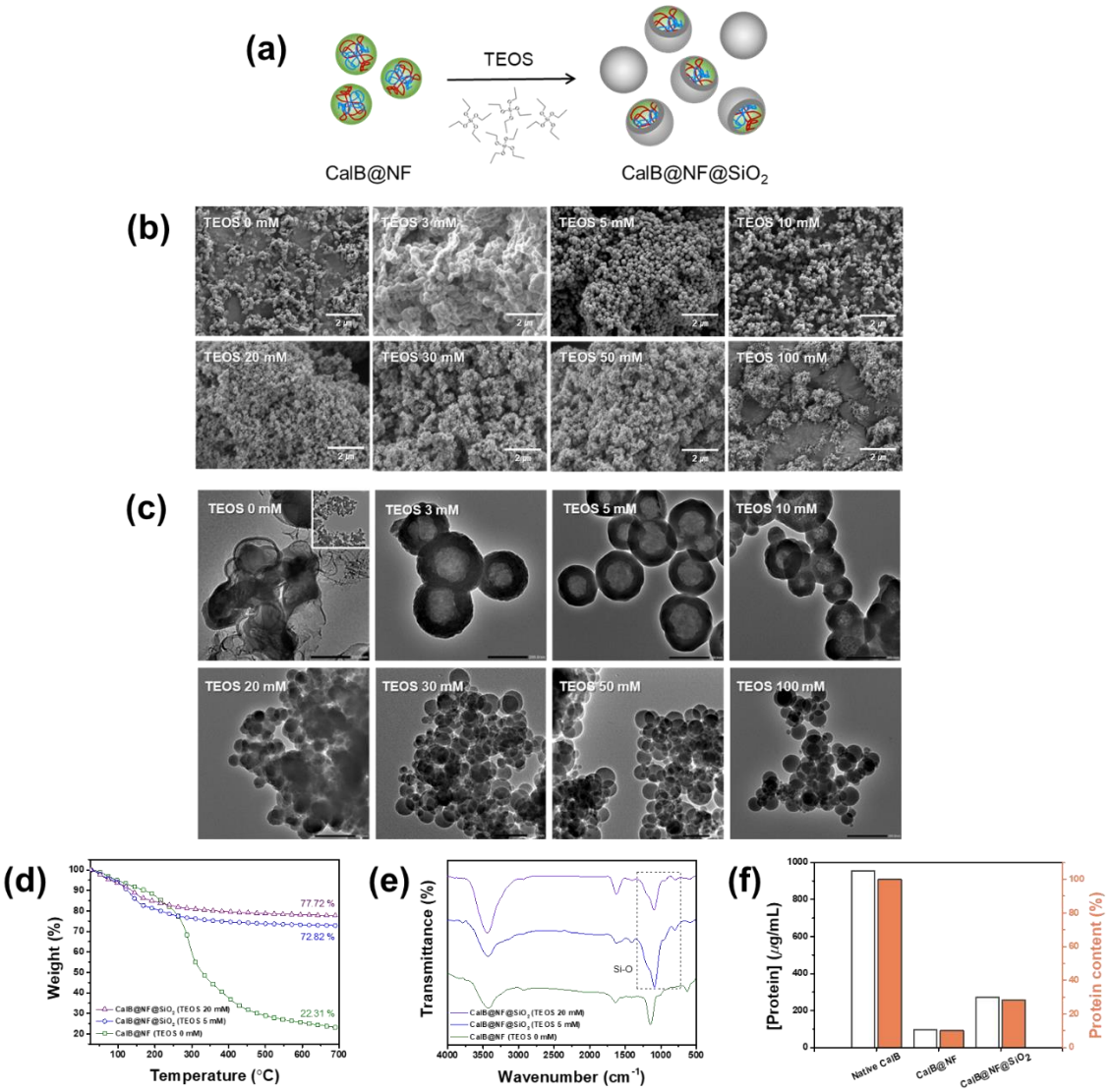

Figure 2. (a) Silica encapsulation process, (b-c) FE-SEM and TEM images of silica encapsulation on CalB@NF as a function of TEOS concentration, (d) TGA analysis, (e) FT-IR spectrum, (f) protein quantification of CalB@NF and CalB@NF@SiO_2 (TEOS 5 mM) by Bradford assay.

The resulting gel network was composed only of silica, forming spherical silica [44]. Therefore, the particle shape of CalB@NF@SiO_2 had a confirmed silica shell and a uniform size, with 5 mM being the most optimal concentration of TEOS. Fig. 2(d) shows amounts of CalB@NF in CalB@NF@SiO_2 at various TEOS concentrations to investigate the amount of CalB@NF for each morphology change via TGA within a temperature range of 25-700 °C. Amounts of CalB@NF at TEOS 5 mM and 20 mM were 50.51% and 55.41%, respectively, compared to that at TEOS 0 mM. Fig. 2(e) shows FT-IR spectra of CalB@NF@SiO_2. Characteristic vibrations of CalB@NF were observed during silica encapsulation. Asymmetric and symmetric stretching vibrations of Si-O-Si bonds were observed at 1080 cm^{-1}, 970 cm^{-1}, and 800 cm^{-1}, indicating that CalB@NF was encapsulated by silica precursor TEOS. Fig. 2(f) shows amounts of CalB enzyme in native CalB, CalB@NF, and CalB@NF@SiO_2 (TEOS 5 mM) according to the Bradford assay. At the same weight, amounts of CalB enzyme for native CalB, CalB@NF, and CalB@NF@SiO_2 (TEOS 5 mM) were 953.5 μg/mL, 94.7 μg/mL, and 270.5 μg/mL, respectively. These results revealed that the amount of encapsulated CalB enzyme in CalB@NF@SiO_2 was three times higher than that of CalB@NF. This result was supported by Fig. 2(d), where amounts of CalB@NF and CalB@NF@SiO_2 (TEOS 5 mM) were 22.31% and 72.82%, respectively, at 700 °C, with a ratio of approximately 1 : 3, which confirmed its reliability. Therefore, the ratio of native CalB : CalB@NF : CalB@NF@SiO_2 (TEOS 5 mM) containing protein was 10 : 1 : 3.

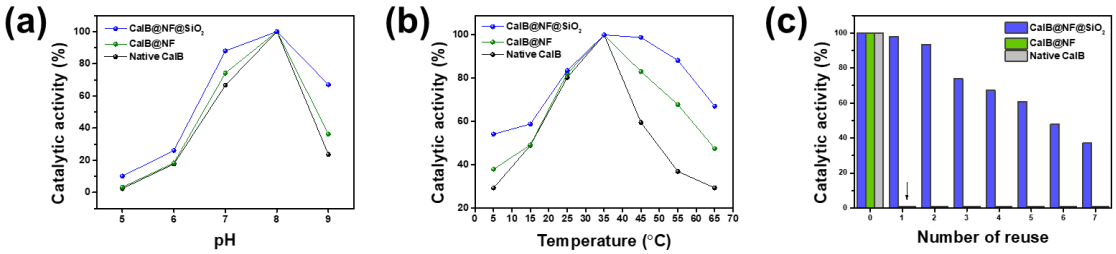

Figure 3. (a) Catalytic activity in different pH and (b) temperature (thermal stability), (c) reusability of native CalB, CalB@NF, and CalB@NF@SiO_2 (TEOS 5 mM).

Fig. 3 shows effects of encapsulation on catalytic activity, pH, thermal stability, and reusability. Catalytic activities of native CalB, CalB@NF, and CalB@NF@SiO_2 (TEOS 5 mM) were evaluated through hydrolysis of PNPB. Fig. 3(a) displays pH dependence of catalytic activities of native CalB, CalB@NF, and CalB@NF@SiO_2 (TEOS 5 mM). All three samples exhibited optimum catalytic activities at pH 8, with reduced activities at other pH values. These results indicate that the catalytic activity is dependent on the enzyme's active state at specific pH values. However, CalB@NF@SiO_2 (TEOS 5 mM) exhibited 10-30% higher catalytic activity than native CalB and CalB@NF under all pH conditions, with pH stability provided by silica encapsulation. Fig. 3(b) shows thermal stability of native CalB, CalB@NF, and CalB@NF@SiO_2 (TEOS 5 mM). All three samples exhibited optimum catalytic activities at 35 °C, with reduced activities at other temperatures.

However, CalB@NF@SiO_2 (TEOS 5 mM) exhibited up to 40% higher catalytic activity than native CalB and CalB@NF under all temperature conditions, with greater differences at higher temperatures. These results were due to silica interfering with protein heat transfer and the superior catalytic activity with thermal stability provided by insoluble silica encapsulation in an aqueous solution. Fig. 3(c) presents reusability of native CalB, CalB@NF, and CalB@NF@SiO_2 (TEOS 5 mM). Native CalB and CalB@NF could not be recovered for evaluation after one use. However, CalB@NF@SiO_2 (TEOS 5 mM) could be recovered and used repeatedly, with reduced catalytic activity after each use. Therefore, enzyme immobilized in silica can be reused repeatedly, increasing process efficiency and reducing costs by continuous use in industrial processes.

Preprints (www.preprints.org) | NOT PEER-REVIEWED | Posted: 16 May 2023 doi:10.20944/preprints202305.1142.v1

Enzymatic hydrolysis was confirmed using native CalB, CalB@NF, and CalB@NF@SiO_2 (TEOS 5 mM) with PNPB as shown in Fig. 4(a). PNPB was hydrolyzed by the enzyme to PNP and butyric acid. Fig. 4(b) shows hydrolysis results of PNPB using native CalB, CalB@NF, and CalB@NF@SiO_2 (TEOS 5 mM) with the same weight and reaction time. PNPB as a reactant exhibited an absorption spectrum at 270 nm, while PNP, the product of PNPB hydrolysis, exhibited an absorption spectrum at 400 nm. Absorbance spectra at 270 nm decreased while those at 400 nm increased for all three samples when using 1 mM of PNPB as a reference.

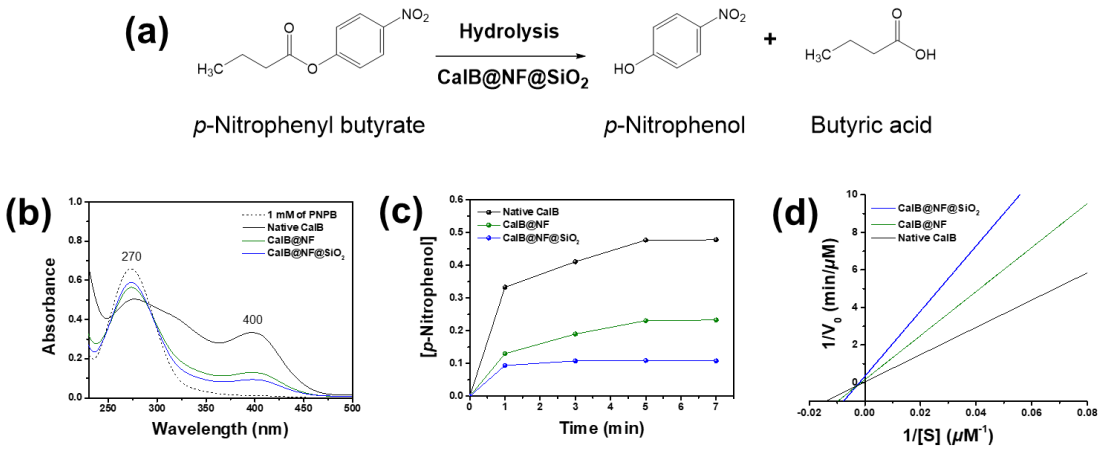

Figure 4. (a) Schemes of enzymatic hydrolysis with CalB@NF@SiO_2 (TEOS 5 mM) against PNPB to PNP, (b) Formed PNP during enzymatic hydrolysis, (c) Absorption spectra of PNP as a function of reaction time, (d) Lineweaver-Burk plots of native CalB, CalB@NF, and CalB@NF@SiO_2 (TEOS 5 mM).

Table 1. Michaelis-Menten parameters of native CalB, CalB@NF, and CalB@NF@SiO_2(TEOS 5 mM) for hydrolysis of PNPB

	K_m (μM)	V_{max} ($\mu M \cdot min^{-1}$)	K_{cat} (min^{-1})	K_{cat}/K_m ($\mu M^{-1} \cdot min^{-1}$)
Native CalB	2,029	27.93	9,484	4,671
CalB@NF	742	6.33	21,473	28,930
CalB@NF@SiO_2	515	2.97	10,065	19,558

These results demonstrate that native CalB, CalB@NF, and CalB@NF@SiO_2 (TEOS 5 mM) can participate in PNPB hydrolysis. Fig. 4(c) shows concentrations of PNP generated during PNPB hydrolysis over time using native CalB, CalB@NF, and CalB@NF@SiO_2 (TEOS 5 mM). Concentrations of PNP for all three samples did not increase after 5 minutes of reaction time, with an order of native CalB > CalB@NF > CalB@NF@SiO_2 (TEOS 5 mM). A high concentration of PNP, the product of PNPB hydrolysis, implied that the reactant PNPB reacted more quickly or extensively with CalB in the catalyst. Thus, the concentration of the product varied depending on the amount and concentration of CalB in the catalyst. Fig. 4(d) shows PNPB enzyme kinetics for native CalB, CalB@NF, and CalB@NF@SiO_2 (TEOS 5 mM) obtained from Lineweaver-Burk plot and Michaelis-Menten kinetics. Enzyme kinetic parameters were calculated. Results are shown in Table 1. The Michaelis-Menten constant (K_m) represents an enzyme's affinity for its substrate, with lower values indicating higher affinity and better binding between the enzyme and substrate. The turnover number (K_{cat}) is a measure of an enzyme's ability to convert substrate into product per unit time. The K_{cat}/K_m ratio has been used as a measure of enzyme performance. K_m values were observed in the order of native CalB > CalB@NF > CalB@NF@SiO_2, with CalB@NF@SiO_2 showing the highest substrate affinity. V_{max} values

Preprints (www.preprints.org) | NOT PEER-REVIEWED | Posted: 16 May 2023 doi:10.20944/preprints202305.1142.v1

were observed in the order of CalB@NF@SiO_2 > CalB@NF > native CalB, in contrast to K_m results. In general, the reaction between a substrate and an enzyme proceeds faster when the enzyme has a higher affinity for the substrate. However, in this study, the high substrate affinity did not result in a correspondingly high reaction rate due to the number of hydroxyl groups on each catalyst surface and in the encapsulated layer. As the hydrolysis reaction occurred in an aqueous solution, the substrate was highly intimate with hydroxyl groups. Therefore, the surface of the silica-encapsulated CalB@NF@SiO_2 synthesized using the sol-gel method contained a large number of hydroxyl groups. CalB@NF was produced using levan, which contained many hydroxyl groups, while native CalB only possessed hydroxyl groups that it originally had. Consequently, the number of hydroxyl groups on the surface of each catalyst was in the order of CalB@NF@SiO_2 > CalB@NF > native CalB. Substrate affinity was also observed in the same order. Moreover, as the CalB@NF@SiO_2 catalyst had an encapsulated layer that did not dissolve in the aqueous solution, the active site that had to directly bind to the substrate was obscured. Although CalB@NF was encapsulated with levan, which dissolved in the aqueous solution, it reacted with the substrate only to the extent that it possessed protein. Therefore, according to results shown in Fig. 2(f), the reaction rate was the highest for native CalB, which had the most protein, and the lowest for CalB@NF@SiO_2, despite having a higher protein content than CalB@NF. This result was also confirmed in Fig. 4(c). The K_{cat} and K_{cat}/K_m ratio related to the enzyme's ability and efficiency were highest for CalB@NF, followed by CalB@NF@SiO_2 and then native CalB. This result was calculated based on K_m and V_{max} values. CalB@NF, which had a high affinity for the substrate due to levan and reacted well with the substrate in the aqueous solution, was the most excellent. Therefore, CalB@NF was the best for enzymatic hydrolysis with the substrate. However, according to results shown in Fig. 3, CalB@NF@SiO_2 was the most convenient for use in harsh environments or continuous processes.

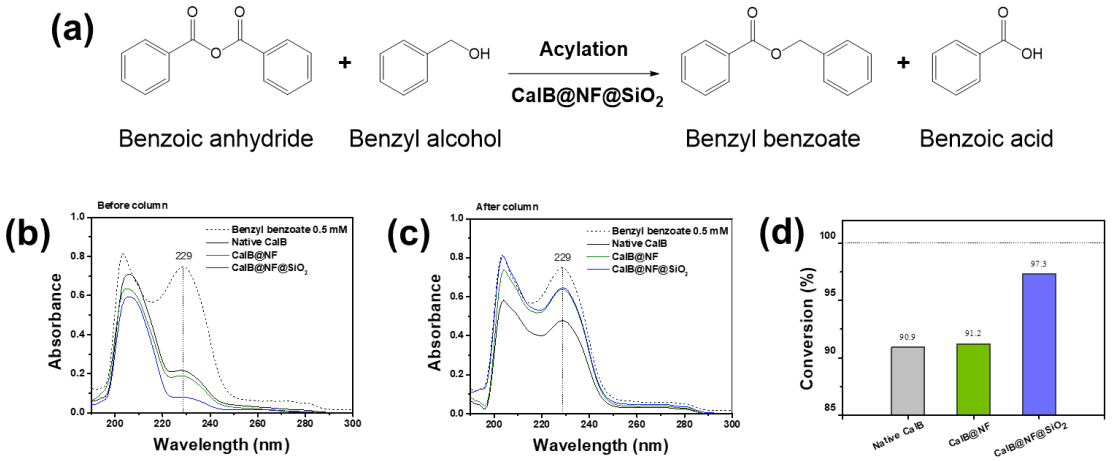

Figure 5. (a) Schemes of enzymatic synthesis for benzyl benzoate, (b-c) Formed benzyl benzoate during enzymatic synthesis before and after column chromatography, (d) Conversion efficiency of benzyl benzoate with native CalB, CalB@NF, and CalB@NF@SiO_2 (TEOS 5 mM).

Fig. 5 shows the process of synthesizing benzyl benzoate through enzymatic synthesis and its conversion efficiency. As shown in Fig. 5(a), enzymatic synthesis of benzyl benzoate using CalB@NF@SiO_2 (TEOS 5 mM) involves reactions using benzoic anhydride as a reactant. In the reaction, benzoic anhydride has two acyl donors, leading to the generation of not only benzyl benzoate (first acyl donor), but also benzoic acid (second acyl donor) when reacting with benzyl alcohol [37,46]. Therefore, benzoic anhydride is suitable for synthesizing benzyl benzoate. According to this phenomenon, benzyl benzoate conversion efficiency was evaluated using native CalB, CalB@NF, and CalB@NF@SiO_2 (TEOS 5 mM). Fig. 5(b) shows results of UV-vis analysis of benzyl benzoate synthesized. Benzyl benzoate showed absorbance at 229 nm. However, it was difficult to distinguish because it was hindered by benzyl alcohol or benzoic acid remaining in the synthesis process.

Preprints (www.preprints.org) | NOT PEER-REVIEWED | Posted: 16 May 2023 doi:10.20944/preprints202305.1142.v1

Therefore, it was separated and purified through column chromatography and analyzed for UV-vis. (Fig. 5(c)). As a result, native CalB, CalB@NF, and CalB@NF@SiO_2 (TEOS 5 mM) all showed benzyl benzoate at 229 nm. Therefore, native CalB, CalB@NF, and CalB@NF@SiO_2 (TEOS 5 mM) were demonstrated for enzymatic synthesis of benzyl benzoate in this process. Fig. 5(d) shows conversion efficiency of benzoic anhydride to benzyl benzoate using native CalB, CalB@NF, and CalB@NF@SiO_2 (TEOS 5 mM). The conversion efficiency was calculated according to the following equation:

$$\text{Conversion } (\%) = \frac{C_i - C_f}{C_i} \times 100$$

In this equation, C_i and C_f were initial and final concentrations of benzoic anhydride before and after enzymatic synthesis, respectively. The conversion efficiency from benzoic anhydride to benzyl benzoate was calculated to be 90.9%, 91.2%, and 97.3% for native CalB, CalB@NF, and CalB@NF@SiO_2 (TEOS 5 mM), respectively. Although conversion efficiencies of native CalB and CalB@NF were similar, that of CalB@NF@SiO_2 (TEOS 5 mM) was found to be almost 100%. This result suggests that silica-encapsulated CalB@NF@SiO_2 (TEOS 5 mM) can prevent a decrease in catalytic activity in organic solvents. Therefore, protein immobilization through silica provides higher stability in organic solvents, resulting in increased catalytic efficiency.

4. Conclusion

CalB@NF@SiO_2 was prepared as a function of TEOS concentration ranging from 3-100 mM. The resulting CalB@NF@SiO_2 showed a uniformly spherical shape depending on TEOS concentration, although particle size and shape varied. The morphology analyzed through TEM revealed the presence of a silica shell at TEOS concentrations of 3-10 mM, while only pure silica was observed at concentrations above 20 mM. CalB@NF@SiO_2 prepared as a function of various TEOS concentrations exhibited the most uniform shape at a TEOS concentration of 5 mM, which demonstrated stability under various pH and temperature conditions. Furthermore, it was confirmed that CalB@NF@SiO_2, but not native CalB or CalB@NF, could be used repeatedly. In addition, enzymatic hydrolysis of PNPB and enzymatic synthesis of benzyl benzoate were proven. Enzymatic hydrolysis showed that PNPB was converted to PNP by Lineweaver-Burk plot and Michaelis-Menten kinetics. Enzymatic synthesis showed that the conversion efficiency of benzyl benzoate corresponding to CalB@NF@SiO_2 (TEOS 5 mM) was 97.3%, indicating that almost all benzoic anhydride was converted to benzyl benzoate. Therefore, CalB@NF@SiO_2 is more stable in aqueous solutions with respect to pH and temperature than native CalB and CalB@NF. In addition, it can be reused. Moreover, it exhibits the highest catalytic efficiency in organic solvents, has less environmental impact, and can be used in continuous processes. Thus, it is expected to greatly reduce costs.

References

[1] S.F. Sousa, Special Issue on “Enzymes as Biocatalysts: Current Research Trends and Applications&rdquo, International Journal of Molecular Sciences 23(24) (2022) 16209.
[2] P.N. Devine, R.M. Howard, R. Kumar, M.P. Thompson, M.D. Truppo, N.J. Turner, Extending the application of biocatalysis to meet the challenges of drug development, Nature Reviews Chemistry 2(12) (2018) 409-421.
[3] I. Thiele, H. Yehia, N. Krausch, M. Birkholz, M.N. Cruz Bournazou, A.B. Sitanggang, M. Kraume, P. Neubauer, A. Kurreck, Production of Modified Nucleosides in a Continuous Enzyme Membrane Reactor, 24(7) (2023) 6081.
[4] P. Fernandes, Miniaturization in Biocatalysis, 11(3) (2010) 858-879.
[5] S. Wu, R. Snajdrova, J.C. Moore, K. Baldenius, U.T. Bornscheuer, Biocatalysis: Enzymatic Synthesis for Industrial Applications, 60(1) (2021) 88-119.
[6] S. Wu, R. Snajdrova, J.C. Moore, K. Baldenius, U.T. Bornscheuer, Biocatalysis: Enzymatic Synthesis for Industrial Applications, 60(1) (2021) 88-119.

Preprints (www.preprints.org) | NOT PEER-REVIEWED | Posted: 16 May 2023 doi:10.20944/preprints202305.1142.v1

[7] J. Ge, D. Lu, Z. Liu, Z. Liu, Recent advances in nanostructured biocatalysts, Biochem. Eng. J. 44(1) (2009) 53-59.
[8] B. Sri Kaja, S. Lumor, S. Besong, B. Taylor, G. Ozbay, Investigating Enzyme Activity of Immobilized Candida rugosa Lipase, J. Food Qual. 2018 (2018) 1618085.
[9] P.P. Chiplunkar, X. Zhao, P.D. Tomke, J. Noro, B. Xu, Q. Wang, C. Silva, A.P. Pratap, A. Cavaco-Paulo, Ultrasound-assisted lipase catalyzed hydrolysis of aspirin methyl ester, Ultrason. Sonochem. 40 (2018) 587-593.
[10] P.B. Juhl, K. Doderer, F. Hollmann, O. Thum, J. Pleiss, Engineering of Candida antarctica lipase B for hydrolysis of bulky carboxylic acid esters, J. Biotechnol. 150(4) (2010) 474-480.
[11] N. Niezgoda, A. Gliszczyńska, Lipase Catalyzed Acidolysis for Efficient Synthesis of Phospholipids Enriched with Isomerically Pure cis-9,trans-11 and trans-10,cis-12 Conjugated Linoleic Acid, Catalysts 9(12) (2019) 1012.
[12] M. Okulus, A. Gliszczyńska, Enzymatic Synthesis of O-Methylated Phenophospholipids by Lipase-Catalyzed Acidolysis of Egg-Yolk Phosphatidylcholine with Anisic and Veratric Acids, Catalysis 10(5) (2020) 538.
[13] X. Li, C. Zhang, S. Li, H. Huang, Y. Hu, Improving Catalytic Performance of Candida rugosa Lipase by Chemical Modification with Polyethylene Glycol Functional Ionic Liquids, Industrial & Engineering Chemistry Research 54(33) (2015) 8072-8079.
[14] T. Siódmiak, G. G. Haraldsson, J. Dulęba, M. Ziegler-Borowska, J. Siódmiak, M.P. Marszałł, Evaluation of Designed Immobilized Catalytic Systems: Activity Enhancement of Lipase B from Candida antarctica, Catalysis 10(8) (2020) 876.
[15] D. Yu, X. Zhang, D. Zou, T. Wang, T. Liu, L. Wang, W. Elfalleh, L. Jiang, Immobilized CALB Catalyzed Transesterification of Soybean Oil and Phytosterol, Food Biophysics 13(2) (2018) 208-215.
[16] A. Kumar, K. Dhar, S.S. Kanwar, P.K. Arora, Lipase catalysis in organic solvents: advantages and applications, Biological Procedures Online 18(1) (2016) 2.
[17] Z. Nazarian, S.S. Arab, Solvent-dependent activity of Candida antarctica lipase B and its correlation with a regioselective mono aza-Michael addition - experimental and molecular dynamics simulation studies, Heliyon 8(8) (2022) e10336.
[18] Q. Wang, R. Zhang, M. Liu, L. Ma, W. Zhang, Co-Immobilization of Lipases with Different Specificities for Efficient and Recyclable Biodiesel Production from Waste Oils: Optimization Using Response Surface Methodology, Catalysis 24(5) (2023) 4726.
[19] R.C. Rodrigues, C. Ortiz, Á. Berenguer-Murcia, R. Torres, R. Fernández-Lafuente, Modifying enzyme activity and selectivity by immobilization, Chem. Soc. Rev. 42(15) (2013) 6290-6307.
[20] U. Guzik, K. Hupert-Kocurek, D. Wojcieszyńska, Immobilization as a Strategy for Improving Enzyme Properties-Application to Oxidoreductases, Molecular 19(7) (2014) 8995-9018.
[21] R.A. Sheldon, S. van Pelt, Enzyme immobilisation in biocatalysis: why, what and how, Chem. Soc. Rev. 42(15) (2013) 6223-6235.
[22] R. DiCosimo, J. McAuliffe, A.J. Poulose, G. Bohlmann, Industrial use of immobilized enzymes, Chem. Soc. Rev. 42(15) (2013) 6437-6474.
[23] F. Secundo, Conformational changes of enzymes upon immobilisation, Chem. Soc. Rev. 42(15) (2013) 6250-6261.
[24] P.V. Iyer, L. Ananthanarayan, Enzyme stability and stabilization—Aqueous and non-aqueous environment, Process Biochem. 43(10) (2008) 1019-1032.
[25] C. Mateo, J.M. Palomo, G. Fernandez-Lorente, J.M. Guisan, R. Fernandez-Lafuente, Improvement of enzyme activity, stability and selectivity via immobilization techniques, Enzyme Microb. Technol. 40(6) (2007) 1451-1463.
[26] R. Srikanth, C.H.S.S.S. Reddy, G. Siddartha, M.J. Ramaiah, K.B. Uppuluri, Review on production, characterization and applications of microbial levan, Carbohydr. Polym. 120 (2015) 102-114.
[27] J.S.C.A. Chidambaram, B. Veerapandian, K.K. Sarwareddy, K.P. Mani, S.R. Shanmugam, P. Venkatachalam, Studies on solvent precipitation of levan synthesized using Bacillus subtilis MTCC 441, Heliyon 5(9) (2019) e02414.
[28] F. Küçükaşik, H. Kazak, D. Güney, I. Finore, A. Poli, O. Yenigün, B. Nicolaus, E.T.J.A.M. Öner, Biotechnology, Molasses as fermentation substrate for levan production by Halomonas sp, Biotechnology and Bioprocess Engineering 89 (2010) 1729-1740.

Preprints (www.preprints.org) | NOT PEER-REVIEWED | Posted: 16 May 2023 doi:10.20944/preprints202305.1142.v1

[29] S. Datta, L.R. Christena, Y.R. Rajaram, Enzyme immobilization: an overview on techniques and support materials, 3 Biotech 3(1) (2013) 1-9.
[30] P. Jampala, M. Preethi, S. Ramanujam, B.S. Harish, K.B. Uppuluri, V. Anbazhagan, Immobilization of levan-xylanase nanohybrid on an alginate bead improves xylanase stability at wide pH and temperature, Int. J. Biol. Macromol. 95 (2017) 843-849.
[31] b. Gabrielly Terassi, B. Cristiani, C. Maria Antonia Pedrine Colabone, IMMOBILIZATION OF LEVANSUCRASE: STRATEGIES AND BIOTECHNOLOGICAL APPLICATIONS, Journal of the Chilean Chemical Society 64(1) (2019).
[32] I. Vīna, A. Karsakevich, M. Bekers, Stabilization of anti-leukemic enzyme l-asparaginase by immobilization on polysaccharide levan, J. Mol. Catal. B: Enzym. 11(4) (2001) 551-558.
[33] H.-Z. Ma, X.-W. Yu, C. Song, Q.-l. Xue, B. Jiang, Immobilization of Candida Antarctica lipase B on epoxy modified silica by sol-gel process, J. Mol. Catal. B: Enzym. 127 (2016) 76-81.
[34] A. Costantini, V. Califano, Lipase Immobilization in Mesoporous Silica Nanoparticles for Biofuel Production, Catalysis 11(5) (2021) 629.
[35] D. Cazaban, A. Illanes, L. Wilson, L. Betancor, Bio-inspired silica lipase nanobiocatalysts for the synthesis of fatty acid methyl esters, Process Biochem. 74 (2018) 86-93.
[36] M. Song, J.H. Chang, Thermally Stable and Reusable Ceramic Encapsulated and Cross-Linked CalB Enzyme Particles for Rapid Hydrolysis and Esterification, Int J Mol Sci 23(5) (2022).
[37] Y. Kuwahara, T. Yamanishi, T. Kamegawa, K. Mori, M. Che, H. Yamashita, Lipase-embedded silica nanoparticles with oil-filled core–shell structure: stable and recyclable platforms for biocatalysts, Chem. Commun. 48(23) (2012) 2882-2884.
[38] L. Betancor, F. López-Gallego, A. Hidalgo, M. Fuentes, O. Podrasky, G. Kuncova, J.M. Guisán, R. Fernández-Lafuente, Advantages of the Pre-Immobilization of Enzymes on Porous Supports for Their Entrapment in Sol−Gels, Biomacromolecules 6(2) (2005) 1027-1030.
[39] S. Escobar, C. Bernal, J.M. Bolivar, B. Nidetzky, F. López-Gallego, M. Mesa, Understanding the silica-based sol-gel encapsulation mechanism of Thermomyces lanuginosus lipase: The role of polyethylenimine, Molecular Catalysis 449 (2018) 106-113.
[40] D.M. Liu, I.W. Chen, Encapsulation of protein molecules in transparent porous silica matrices via an aqueous colloidal sol–gel process, Acta Mater. 47(18) (1999) 4535-4544.
[41] K. Kang, J. Choi, J.H. Nam, S.C. Lee, K.J. Kim, S.-W. Lee, J.H. Chang, Preparation and Characterization of Chemically Functionalized Silica-Coated Magnetic Nanoparticles as a DNA Separator, The Journal of Physical Chemistry B 113(2) (2009) 536-543.
[42] M.M. Bradford, A rapid and sensitive method for the quantitation of microgram quantities of protein utilizing the principle of protein-dye binding, Anal. Biochem. 72(1) (1976) 248-254.
[43] T. Zor, Z. Selinger, Linearization of the Bradford Protein Assay Increases Its Sensitivity: Theoretical and Experimental Studies, Anal. Biochem. 236(2) (1996) 302-308.
[44] V. Selvarajan, S. Obuobi, P.L.R. Ee, Silica Nanoparticles—A Versatile Tool for the Treatment of Bacterial Infections, Frontiers in Chemistry 8 (2020).
[45] A.C. de Meneses, M. Balen, E. de Andrade Jasper, I. Korte, P.H.H. de Araújo, C. Sayer, D. de Oliveira, Enzymatic synthesis of benzyl benzoate using different acyl donors: Comparison of solvent-free reaction techniques, Process Biochem. 92 (2020) 261-268.